World Scientific
www.worldscientific.com

STRUCTURE AND ELECTRICAL PROPERTIES OF SrO-BOROVANADATE $(V_2O_5)_z(SrO)_{0.2}(B_2O_3)_{0.8-z}$ GLASSES

A. MEKKI[*,†], G. D. KHATTAK[†] and M. N. SIDDIQUI[‡]

[†]*Physics Department, King Fahd University of Petroleum & Minerals,*
Dhahran 31261, Saudi Arabia
[‡]*Chemistry Department, King Fahd University of Petroleum & Minerals,*
Dhahran 31261, Saudi Arabia
[*]*akmekki@kfupm.edu.sa*

SrO-borovanadate glasses with the nominal composition $(V_2O_5)_z(SrO)_{0.2}(B_2O_3)_{0.8-z}$, $0.4 \leq z \leq 0.8$ were studied by direct current (DC) electrical conductivity, inductively coupled plasma (ICP) spectroscopy, Fourier transform infrared (FT-IR) spectroscopy and X-ray-powder-diffraction (XRD). These glasses were prepared by a normal quench technique and the actual compositions of the glasses were determined by ICP spectroscopy. XRD patterns confirm the amorphous nature of the present glasses. The temperature dependence of DC electrical conductivity of these glasses has been studied in terms of different hopping models. The IR results agree with previous investigations on similar glasses and it has been concluded that similar to SrO-vanadate glasses, metavanadate chainlike structures of SrV_2O_6 and individual VO_4 units also occur in these SrO-borovanadate glasses. The SrV_2O_6 and VO_n polyhedra predominate in the low B_2O_3 containing SrO-borovanadate glasses as the B substitutes into the V sites of the various VO_n polyhedra and only when the B_2O_3 concentration exceeds the SrO content do BO_n structures appear. This qualitative picture of three distinct structural groupings for the Sr-vanadate and Sr-borovanadate glasses is consistent with the proposed glass structure on previous IR and extended X-ray absorption fine structure (EXAFS) studies on these types of glasses. The conductivity results were analyzed with reference to theoretical models existing in the literature and the analysis shows that the conductivity data are consistent with Mott's nearest neighbor hopping model. However, both Mott VRH and Greaves models are suitable to explain the data. Schnakenberg's generalized polaron hopping model is also consistent with the temperature dependence of the activation energy, but the various model parameters such as density of states, hopping energy obtained from the best fits were found to be not in accordance with the prediction of the Mott model.

Keywords: SrO-borovanadate glasses; semiconducting glasses; IR spectra; electrical conductivity.

PACS numbers: 61.10.Nz, 61.14.Qp, 61.43.Fs, 61.82.Fk, 71.23.Cq, 72.15.Cz

1. Introduction

Semiconducting glasses can be generally divided into two groups, chalcogenide glasses and oxide glasses containing transition metal (TM) ions such as Fe, Co, V, Cu, etc. Studies of oxide glasses containing moderate to large concentration of TM oxides continue to be of potential technological interest because of their semiconducting properties. The electrical conduction in these glasses has been interpreted by the small polaron hopping model where the conduction properties arise from electron hopping between two TM ions having different valence states.[1–3] Since the unpaired electron induces a polarization around the TM ion, conduction can be described in terms of a model based on polarons. However, a more detailed modeling of the conduction process is limited because of numerous material factors including the type and concentration of the TM ion, the number of valence states associated with the TM ion, the glass preparation conditions, and the microstructures within the glass matrix. Thus, information on the structure of a glass is imperative for further elucidating our understanding of the glass properties.

Transition-metal (TM) oxide glasses have been frequently studied from both a mechanical and physical point of view in order to better understand the transport mechanism in these semiconducting glasses.[4,5] Direct current (DC) conductivity of vanadium oxide glasses in which V_2O_5 is associated with other glass formers such as TeO_2, As_2O_3, P_2O_5 has been extensively studied and these studies have shown that the "small poloron" model can be used to describe the electronic transport phenomena in these materials. Very few studies have been carried out on glasses containing B_2O_3 and V_2O_5. These glasses have their potential applications as optical and electrical memory switching, cathode materials for making solid devices and optical fibre.[6,7] Direct current (DC) electrical conductivity and IR studies were carried out in a continuation of our previous work "X-ray Photoelectron Spectroscopy (XPS) and Magnetization Studies of Strontium-Borate Vanadate Glasses"[8] in an attempt to understand the nature of the mechanism governing the DC conductivity and the effect of addition of V_2O_5 on the electrical properties in these glasses. From the analysis of the XPS spectra for the Sr $3p$, B $1s$, V $2p$, and O $1s$ core levels, several distinct concentration regimes were identified in terms of various structural units being present. The ratios of V^{4+}/V_{total} and NBO/O_{total} (NBO stands for nonbridging oxygen) were determined from V $2p$ and O $1s$ spectra of these glasses. In the present work the effect of the V_2O_5 content and the ratios of V^{4+}/V_{total} and NBO/O_{total} in SrO-borovanadate glasses has been examined on the electrical and structural properties of the glasses with the help of Fourier transform infrared (FT-IR) spectroscopy and the DC conductivity studies as explained in Sec. 3 of the text.

2. Experimental Methods

2.1. *Sample preparation*

The glasses investigated in this paper were prepared by melting dry mixtures of reagent grade V_2O_5, B_2O_3 and SrO in alumina crucibles with nominal compositions

$(V_2O_5)_z(SrO)_{0.2}(B_2O_3)_{0.8-z}$, $0.4 \leq z \leq 0.8$. Since the oxidation and reduction reactions in a glass melt are known to depend on the size of the melt, on the sample geometry, on whether the melt is static or stirred, on thermal history and on quenching rate, all glass samples were prepared under similar conditions to standardize these factors. Approximately 30 g of chemicals were thoroughly mixed to obtain a homogenized mixture for each V_2O_5 concentration. The crucible containing the batch mixture was then transferred to an electrically heated melting furnace maintained at 1000–1100°C depending on the composition of the sample. The melt was left for about an hour under atmospheric conditions in the furnace during which the melt was occasionally stirred with an alumina rod. The homogenized melt was then cast onto a stainless steel plate mold to form glass disks of approximately 1.5 cm diameter and 3 mm thickness for DC conductivity measurements. After casting, the specimens were annealed at 200°C for two hours. X-ray powder diffraction patterns indicated that the glasses formed were completely amorphous. After preparation, the samples were stored in a vacuum desiccator to minimize any further oxidation of the glass samples. The actual compositions of the glasses were determined by inductively coupled plasma spectroscopy (ICP) and are listed in Table 1.

2.2. *Measurement techniques*

2.2.1. *DC conductivity*

For measuring DC conductivity, disc-shaped samples of diameter 1.5 cm and thickness 3.0 mm were made, polished and then the evaporation of gold electrodes on polished surfaces was carried out in vacuum. Measurements of DC conductivity as a function of temperature, in all the samples, were made by two probe technique. A constant voltage was applied and the current was measured in a temperature range 293–473 K. No overheating of the sample was observed when the voltage was applied. To obtain the variation of conductivity with temperature, the sample was placed in a furnace, brought to the desired temperature and maintained at that temperature for sufficient time before taking the measurements to ensure thermal stability. Further, our claim of the thermal stability was supported by the fact that the data was reproducible when the measurements were repeated on cooling down the sample slowly. The temperature was measured by a Pt/Pt-10% Rh

Table 1. Nominal and actual molar composition of SrO-borovanadate $(V_2O_5)_z(SrO)_{0.2}(B_2O_3)_{0.8-z}$ glasses.

Nominal	SrO	B_2O_3	V_2O_5
$z = 0.4$	0.214	0.395	0.391
$z = 0.5$	0.198	0.3–7	0.495
$z = 0.6$	0.203	0.211	0.586
$z = 0.7$	0.192	0.118	0.690
$z = 0.8$	0.206	—	0.794

thermocouple. From the conductivity versus temperature data, the values of different parameters were obtained using different theoretical models as explained in Sec. 4.

2.2.2. *X-ray diffraction (XRD)*

X-ray diffraction (XRD) patterns of the samples were recorded using a Shimadzu XRD-6000 X-ray diffractometer using a Cu anode (K_α, $\lambda = 1.5418$ Å).

2.2.3. *Infrared spectra (IR)*

Infrared spectra (IR) were recorded on a Perkin Elmer Model 16F PC FT-IR spectrophotometer loaded with Spectrum v2.00 software (Massachusetts, USA). Sample pellets for various glasses were prepared for FT-IR measurements by mixing approximately 1–2 mg of the glass powder with about 100–150 mg of spectroscopic grade KBr powder and grinding the mixture to a very fine powder and then compressing the mixture in an evacuable die under 10,000 pound pressure. The KBr powder was dried at 110°C and allowed to cool in a vacuum desiccator prior to making the pellets, to avoid adsorption of the moisture. All IR spectra of samples were recorded in the range of 400–4000 cm^{-1} using the following settings: number of scans 4; gain 1; apodization weak; OPD Velocity 0.3 cm/s; and resolution 4.

3. Results and Discussion

3.1. *X-ray diffraction*

The amorphous nature of the samples was confirmed from X-ray diffraction (XRD). The XRD patterns for the glasses are shown in Fig. 1. The figure exhibits a broad diffuse scattering at low angles instead of crystalline peaks confirming a long-range structural disorder characteristic of amorphous network, i.e., XRD patterns indicated glassy behavior with a broad hump at $2\theta = 25° - 27°$ with the observation of no peak corresponding to V_2O_5 indicating that V_2O_5 has completely entered the glass matrix and that the glasses formed were completely amorphous.

3.2. *FT-IR spectra*

Infrared spectroscopy has proved to be an important tool for the investigation of structure and dynamics of disorder materials. IR spectra of materials are a sensitive function of composition and may help to get the idea of the nature of vibration in a disorder system. The room temperature vibration spectra of the glasses were obtained. Although infrared spectra were recorded in the wider range of 400–4000 cm^{-1} but the range of 400–2000 cm^{-1} for all glasses was selected and shown in Fig. 1 and Table 2. This is the finger-printing range of primary interest as no significant changes are observed beyond 2000 cm^{-1} and also spectra from 2000 cm^{-1}

Table 2. Characteristic infrared absorptions peaks (cm^{-1}) for V_2O_5, B_2O_3, SrO, SrO-borovanadate $(V_2O_5)_z(SrO)_{0.2}(B_2O_3)_{0.8-z}$ glasses.

Series										
V_2O_5		1502 s		1190 s	1019 mp		845–805 bp			594–473 small peaks
SrO	1699		1458		1026		855		600–585 broad	450–409 small peaks
B_2O_3		1505–1352 bp		1192, 1137 sp	1037 sh and 1008 sp	948 sp	806–771 bp	694 sp	646–467 small peaks	
$z = 0.4$	1644		1453	1258	1181 sh	971–890	810–418 bs			
$z = 0.5$	1652	1551 Different	⋯	⋯	⋯	971	SAME			
$z = 0.6$	1645	1551	1455 sh	1256	1181 sp	1021 ob and 971	SAME			
$z = 0.7$	1647	1551, 1507	1451	1256	⋯	971	SAME			
$z = 0.8$	1645	1551	1447	⋯	⋯	971	SAME			

s (small), sp (sharp peaks), mp (main peak), bp (broad peak), ob (obvious but small), sh (shoulder), bs (bunch of small peaks)
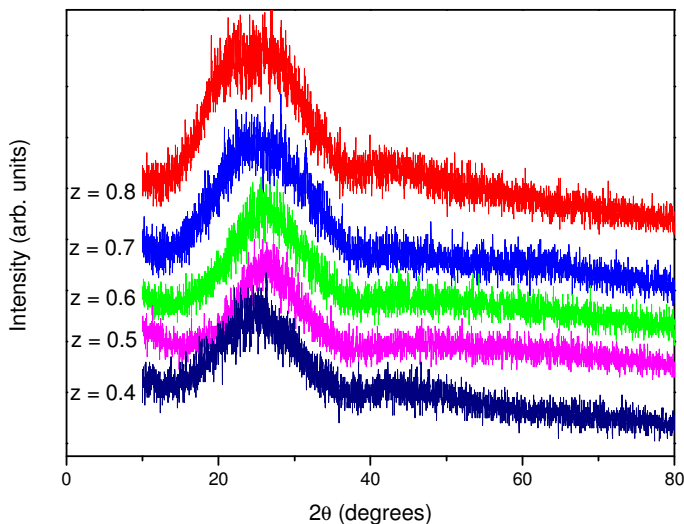
Fig. 1.   XRD for different glass composition of SrO-borovanadate $(V_2O_5)_z(SrO)_{0.2}(B_2O_3)_{0.8-z}$ glasses at room temperature.

towards higher numbers look the same for all compositions. For comparison, spectra are also shown for V_2O_5 and SrO in Fig. 1 and Table 2.

3.2.1. *IR for pure B_2O_3*

The transmission peaks observed for B_2O_3 are shown in Fig. 2 and Table 2 as follows: 1505–1352 cm^{-1} (a broad peak), 1190–1137 cm^{-1} (small peaks but sharp), 1008 cm^{-1}, 948 cm^{-1} (sharp peaks), 806–771 cm^{-1} (broad peak), and a sharp peak at 694 cm^{-1}. There are small peaks in the region 646–467 cm^{-1}. The presented IR spectrum for B_2O_3 shows quite a good match with that reported in the literature.[9]

3.2.2. *IR for pure V_2O_5*

As seen from Fig. 2, peaks were recorded at 1019 cm^{-1} (main peak used in the discussion), 845–805 cm^{-1} (broad peak), broad band from 594 cm^{-1} to 470 cm^{-1} together with small bumps at 1502 cm^{-1} and 1190 cm^{-1}. Our data agrees quite well with that shown in the literature[10] where peaks have been observed at 1020 cm^{-1}, 810 cm^{-1}, 600 cm^{-1} and 480 cm^{-1}.

3.2.3. *IR for pure SrO*

For SrO powder peaks were recorded at 1699 cm^{-1}, 1458 cm^{-1}, 1026 cm^{-1}, 855 cm^{-1} with broad bands from 585 cm^{-1} to 600 cm^{-1} and 409 cm^{-1} to 450 cm^{-1} as shown in Table 2.
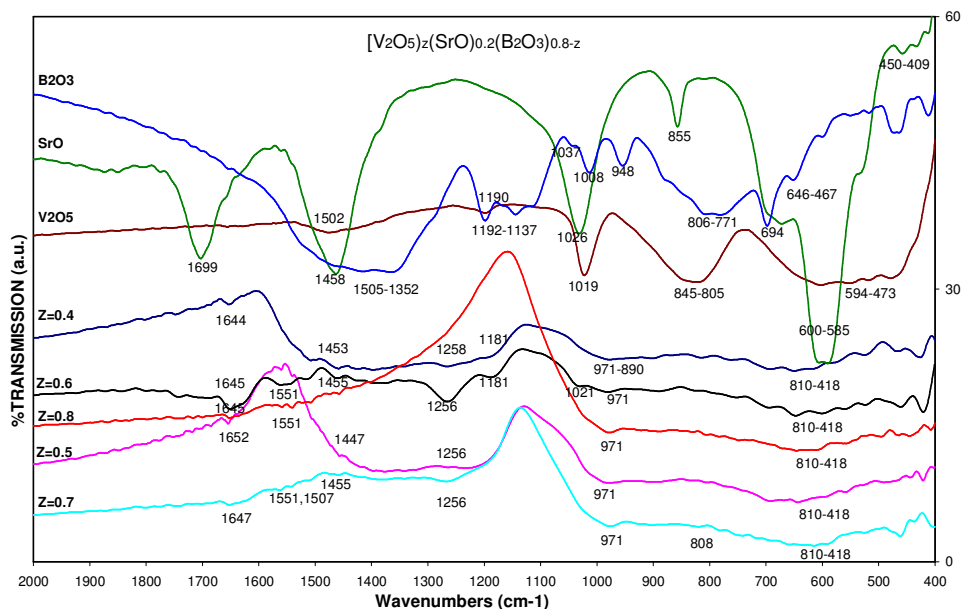
Fig. 2.   IR spectra for SrO-borovanadate $(V_2O_5)_z(SrO)_{0.2}(B_2O_3)_{0.8-z}$ glasses, V_2O_5, B_2O_3 and SrO oxides at room temperature.

3.2.4. *Main features of IR spectra for Sr-borovanadate glasses* $(V_2O_5)_z(SrO)_{0.2}\ (B_2O_3)_{0.8-z}$
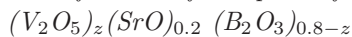
Infrared spectra studies have been carried out on powdered samples dispersed in KBr pellets and shown in Fig. 2 for the range of 400–2000 cm^{-1}. A peak was observed at 1646 cm^{-1} for all glasses and is independent of the concentration of the constituents of the glasses. The origin of these peaks is not obvious, but the —OH bending mode gives rise to absorption in this region and the possibility of some adsorbed water giving rise to these peaks cannot be ruled out. Hence the peak observed at 1600 cm^{-1} is possibly due to the hygroscopic nature of the powdered samples. Further, this peak is obtained in all the glasses almost at the same position.

The strong band observed for V_2O_5 at 1019 cm^{-1} which was reported at 1020 cm^{-1} by previous studies,[11] carried out on SrO-vanadate glasses, has been assigned to the vibration of the isolated V=O non-bridge bonds in the VO$_5$ trigonal bipyramids.[12] With the addition of SrO, changes are observed in the spectra. In the case of SrO-vanadate glasses with SrO content 20–30%, band at 968 cm^{-1} is observed with reduced intensity in the spectra (a shoulder is also observed at 968 cm^{-1} for SrO content 40%) and for glasses with SrO content 30, 40, and 50% a band at 886 cm^{-1} is observed but this band is missing from IR spectrum for glass containing 20% SrO.[13] Further, it is observed that the band around 1020 cm^{-1} completely vanishes for these glasses, suggesting that the isolated V=O bonds might have vanished or become too weak to be detected.

The IR spectra for the SrO-borovanadate glasses arise largely from the modified borate networks. According to previous studies,[14] the structure of the boron oxide glass consists of a random network of planer BO_3 triangles with a certain fraction of six-membered (boroxol) rings. X-ray and neutron diffraction data suggests that glass structure consists of a random network of BO_3 triangles without boroxol rings. Also (Fig. 2) the absence of peak around 806 cm^{-1} indicates that borate network does not contain any boroxol rings.[15] By looking at the IR spectra, Fig. 2 and Table 2, the vibrational modes of the borate network are seen to be active in four IR spectral regions, which are similar to those previously reported.[16]

(i) The first group of bands which occur from 1200 cm^{-1} to 1500 cm^{-1} is due to the asymmetric stretching relaxation of the B—O bond of triangle BO_3 units.
(ii) The second group lies between 900 and 1200 cm^{-1} and is due to the B—O bond stretching of the tetrahedral BO_4 units.
(iii) The third group is around 800 and 900 cm^{-1} and is due to the bending of B—O—B linkages in borate networks.
(iv) Below 800 there are several peaks in B_2O_3, V_2O_5 and SrO and are retained in all these glasses.

In the present work, we try to investigate the effect of addition of V_2O_5 while keeping the content of SrO fixed at 20% in these SrO-borovanadate glasses. With the addition of V_2O_5, the IR spectra changes and new bands are observed in the region 1200 to 1400 cm^{-1} (Fig. 2 and Table 2). A small peak is observed at around 971 cm^{-1} for all glasses. Further, for $z = 0.6$ glass, a peak around 1021 cm^{-1} is also observed in addition to the peak at 971 cm^{-1}, suggesting that the isolated V=O bonds might have vanished or become too weak to be detected for the other glasses.

The bands observed at 1181 cm^{-1} for the two glasses with $z = 0.4$ and 0.6 are probably due to the shifting of the band at 1192 cm^{-1} observed for pure B_2O_3 but missing from the other glasses. The IR results agree with previous investigations on similar glasses, and it has been concluded that similar to SrO-vanadate glasses, metavandate chainlike structures of SrV_2O_6 and individual VO_4 units also occur in SrO-borovanadate glasses. The SrV_2O_6 and VO_n polyhedra predominate in the low B_2O_3 containing SrO-borovanadate glasses as the B substitutes into the V sites of the various VO_n polyhedra and only when the B_2O_3 concentration exceeds the SrO content do BO_n structures appear. This qualitative picture of three distinct structural groupings for the Sr-vanadate and Sr-borovanadate glasses is consistent with the proposed glass structure on previous IR and extended X-ray absorption fine structure (EXAFS) studies[17,18] on these types of glasses. However, the question remains as to whether the oxygens surrounding the boron ions have binding energies or environments similar to that of the higher binding energy bridging oxygen in the VO_5 polyhedra, or are more representative of the lower binding energy non-bridging oxygen.

Structure investigations of borovanadate glasses are less numerous than those for the vanadate glasses. Recently Raman and EXAFS spectroscopic techniques[17,18]

have been used to determine the structure of borovanadate glasses with ZnO and Li$_2$O dopants. The ZnO-borovanadate glasses, which are probably more similar to our SrO-borovanadate glass series, found VO$_4$ to be the predominated polyhedra with the symmetry around the V^{5+}-ions being more distorted in comparison to the crystalline materials. With increasing V$_2$O$_5$ content relative to B$_2$O$_3$, the distorted VO$_4$ tetrahedra would initially be incorporated into the borate groupings of the BO$_3$ and BO$_4$ units. At higher concentrations, these metavanadate groups could be connected to each other directly, forming possibly metavanadate chain structures. Moreover, the Stevels' structural parameter decreases with the incorporation of VO$_4$, and thus indicates a reduction in the average number of bridging oxygen per network-forming polyhedron.[17] Another structural study of the strontium borate glass system[19] indicates that the Sr ions act only as a network modifier with a coordination number of six as determined from the EXAFS measurements. Based on these studies, we can state that the local structure of the Sr-borovanadate glasses is quite similar to the Sr-vanadate glasses except that BO$_3$ polyhedra are substituted for the VO$_n$ polyhedral units.

It may be appropriate to mention that similar to the Sr-vanadate glass series, from our XPS studies[8] the experimentally normalized peak areas under the lower binding energy O $1s(1)$ peak for the entire Sr-borovanadate glass series are found to be in reasonably good agreement[8] with a formula where NBO depends only on the SrO and V$_2$O$_5$ content.

3.3. *DC electrical conductivity*

The temperature dependence of dc electrical conductivity, σ, for these glasses is shown in Fig. 3 as plots of Log (σ) versus 1000/T. It is observed in the figure that the conductivity is almost activated for the temperature range of measurements as the variation of the activation energy with temperature is not significant over the entire temperature range of measurements. This dependence of the dc conductivity obeys the well-known Arrhenius formula

$$\sigma = \sigma_o \text{Exp}[-W/k_B T] \tag{1}$$

where "W" is the activation energy for hopping conduction. The pre-exponential factor, σ_o, contains several constants including the vibrational frequency of the ions and k_B is the Boltzmann constant.

The values of "W" were calculated by fitting the experimental data to the equation

$$\text{Log}\,\sigma = \text{Log}\,\sigma_o - (W/1000 k_B T)(1000/T)(1/2.303) \tag{2}$$

The activation energy W (eV) and the values of Log σ $(\Omega - m)^{-1}$ at 400 K are shown in Table 3 for SrO-borovanadate glasses. The variation in dc electrical conductivity, σ, and the activation energy, W, as a function of vanadium content is shown in Fig. 4 for these glasses. It is evident that, generally, dc electrical conductivity increases while the activation energy decreases with the addition of vanadium
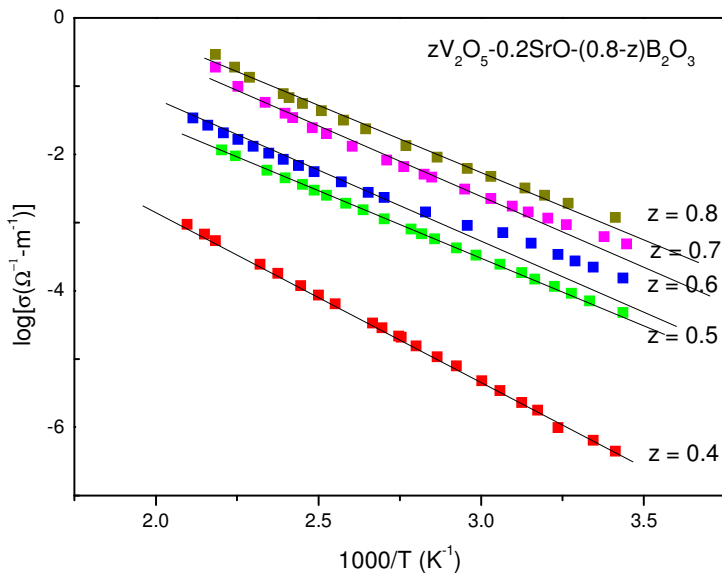
Fig. 3. Temperature dependence of dc conductivity, σ, for SrO-borovanadate $(V_2O_5)_z(SrO)_{0.2}(B_2O_3)_{0.8-z}$ glasses as plots of Log σ as a function of 1000/T. The solid lines are the least-square fits to the data.

Table 3. Activation energy W (eV) and Log σ $(\Omega - m)^{-1}$ at 400 K for SrO-borovanadate $(V_2O_5)_z(SrO)_{0.2}(B_2O_3)_{0.8-z}$ glasses.

Nominal	W (eV)	Log σ $(\Omega - m)^{-1}$	T_{cal} (K)*	NBO/TO**	V^{4+}/V_{total}**
$z = 0.4$	0.503	−4.044		0.635	0.0283
$z = 0.5$	0.383	−2.547	452	0.649	0.0276
$z = 0.6$	0.340	−2.227		0.754	0.1007
$z = 0.7$	0.388	−1.586		0.808	0.0721
$z = 0.8$	0.390	−1.293		0.860	0.0427

*Theoretical slope $(\tan \theta = -1/2.303 \, k_B T)$
**From reference (Khattak *et al. Phys. Rev. B*)

oxide content in the glass composition. It has been observed previously[20] that the decrease in the activation energy is sudden for ionic conductivity while for electronic conductivity the change is somewhat exponential. Hence this behavior is a feature of small polaron hopping (SPH)[21,22] and the decrease of W with increasing concentration of V_2O_5 can be attributed to the decrease in V—V spacing.[21]

Generally, these types of glasses exhibit mixed electronic (via electrons hopping along V^{4+}—O—V^{5+} paths) and ionic (via Sr^{2+} ions) conductivity and glasses with such mixed electrical conductivity attract scientific interest because they are of both academic and commercial potential applications. To obtain evidence for the nature of these two types of conduction, the time effect of the voltage (100 V DC) on the electrical conductivity of glasses was studied at a temperature of 150°C. Over a
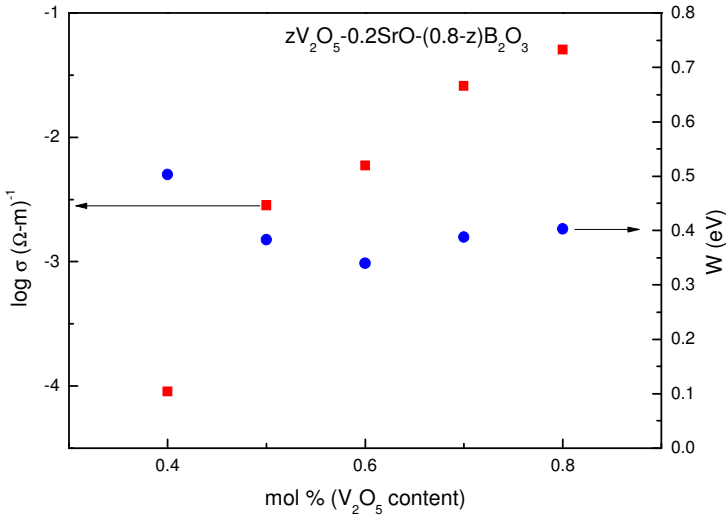
Fig. 4.   Dependence of dc conductivity, $\sigma(\blacksquare)$, and activation energy, $W(\bullet)$, on the V_2O_5 content for SrO-borovanadate $(V_2O_5)_z(SrO)_{0.2}(B_2O_3)_{0.8-z}$ glasses.

period of an hour, no appreciable change was observed in the conductivity. This indicates that the conduction can be considered as electronic in nature. Further, it is known that the ionic conductivity increases as a result of breakdown of the bridging oxygen (BO) bonds and formation of non-bridging oxygen ions.[23] This produces the so-called open structure, through which the charge carriers can move with higher mobility. In our case it is observed that all these three quantities NBO/O_{total}, V^{4+}/V_{total} and DC conductivity increase with an increase in the vanadium content [8, Table 3] but we do not observe any change in the DC conductivity with time which also suggests that the conductivity depends only on the ratio of V^{4+}/V_{total} and hence the presence of electronic conductivity.

Mostly studies have been concerned with the dependence of the electrical conductivity on the V_2O_5 content and the V^{4+}/V^{5+} ratio. In their study of the electrical properties of glasses of the systems $CaO-B_2O_3-V_2O_5$ and $CaO-P_2O_5-V_2O_5$, Kennedy and Mackenzie[24] indicated that for similar compositions and similar V^{4+}/V^{5+} ratios, the conductivity of borate glasses is lower than that of phosphate glasses. They deduced that the network former has a great effect on the electrical conduction of such glasses.

In Mott's model[21,25] for conduction process in the TMO glasses, the conduction mechanism is considered in terms of phonon-assisted hopping of small polarons between localized states. According to this model, the DC conductivity for the nearest–neighbor hopping in non-adiabatic regime at high temperatures $(T > \theta_D/2)$ is given by

$$\sigma = \frac{\nu_o N e^2 R^2}{k_B T} C(1-C) \exp(-2\alpha R) \exp\left(-\frac{W}{k_B T}\right) \tag{3}$$

where ν_o is the longitudinal optical phonon frequency, C is the fraction of reduced vanadium ions, V^{4+}/V_{total}, α^{-1} is the localization length for the wave function, R is the average hopping distance, k_B is the Boltzmann constant, e is the electronic charge and w is the activation energy for hopping conduction.

The activation energy for the hopping conduction is given by[3]

$$W = W_D + W_H/2 \quad \text{for } T > \theta_D/2$$
$$W \approx W_D \qquad\qquad \text{for } T < \theta_D/4$$

where W_H is the hopping energy, W_D is the energy difference between two adjacent sites i.e., disorder energy and θ_D is the Debye temperature.

In the framework of Mott's model, the nature of the polaron hopping mechanism in the high temperature range (adiabatic or non-adiabatic), where an activated behavior of the conductivity was observed, can be ascertained from the plot of Log σ versus activation energy, W, at an arbitrary experimental temperature in this range. It has been suggested[21,26] that the hopping would be in the adiabatic regime if the temperature estimated, T_c, from the slope of such a plot were close to the experimental temperature, T. Otherwise, the hopping would be in the non-adiabatic regime. A plot of Log σ at 400 K versus W is shown in Fig. 5 for these glasses. It is evident from this figure that the plot is not linear, the data is very scattered and thus an estimation of temperature and hence the determination of the nature of the hopping mechanism is not reliable. However, we have tried to fit the data into a straight line and the temperature calculated, T_c, from the fitted line is very different from the experimental temperature chosen (400 K) [Table 3]. This may suggest that the conduction mechanism in the present glasses maybe due to non-adiabatic hopping of the polarons.[21,25]
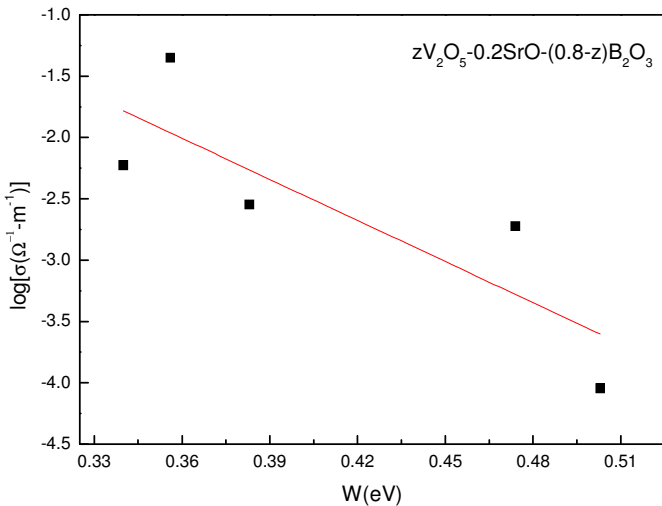
Fig. 5. A plot of Log σ versus W for SrO-borovanadate $(V_2O_5)_z (SrO)_{0.2} (B_2O_3)_{0.8-z}$ glasses at 400 K.

The experimental results were analyzed with reference to theoretical models existing in the literature.

(i) Greaves variable range hopping (VRH) model: According to this model,[27] the expression for the conductivity can be written as

$$sT^{1/2} = A \operatorname{Exp}(-B/T^{1/4}) \qquad (4)$$

where A and B are constants. The values of A and B can be obtained from the intercept and slope, respectively, of the plot Log $(\sigma T^{1/2})$ versus $T^{-1/4}$. Further, the value of B can be written

$$B = 2.1[\alpha^3/k_B N(E_F)]^{1/4} \qquad (5)$$

Figure 6 shows the plots of Log $(\sigma T^{1/2})$ versus $T^{-1/4}$ and the linear relationship confirms the Greaves VRH model.[27] The values of parameters A and B obtained from these curves are given in Table 4. Values of the density of states at the Fermi level, $N(E_F)$, were estimated from Eq. (5) assuming $\alpha = 33 \ nm^{-1}$[28] and shown in Table 4. These values are consistent with those of the usual semiconducting oxide glasses[29,30] suggesting that this model is suitable to explain the conductivity data. Thus, it is concluded that the appearance of the VRH for the temperature interval of measurements, $T = 293 - 470$ K is reasonable for the present glasses.

(ii) At lower temperatures, where polaron binding energy is very small and disorder energy, W_D, plays a dominant role in the conduction mechanism, Mott and Davis[31] have shown that hops may occur preferentially beyond nearest neighbors. The conductivity for the so-called variable range hopping (VRH) mechanism is
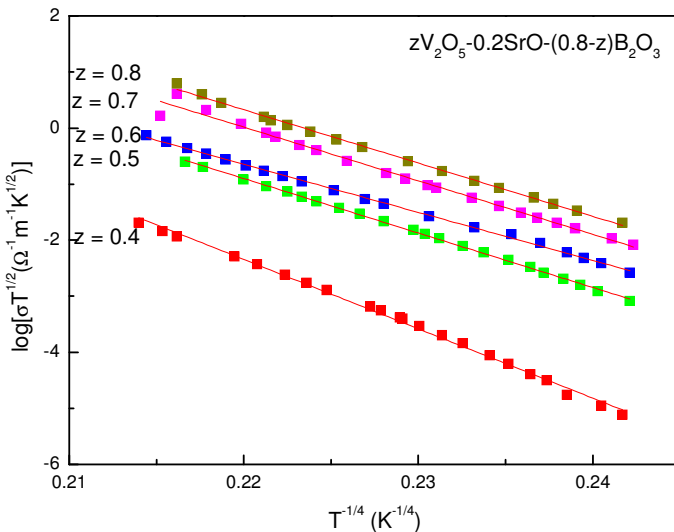
Fig. 6. A plot of Log $(\sigma T^{1/2})$ versus $T^{-1/4}$ for SrO-borovanadate $(V_2O_5)_z(SrO)_{0.2}(B_2O_3)_{0.8-z}$ glasses. The solid lines are the best fits to Eq. (4).

Table 4.   Parameters A, B, $N(E_F)$ obtained for Greaves variable-range hopping conduction[**] for SrO-borovanadate $(V_2O_5)_z(SrO)_{0.2}(B_2O_3)_{0.8-z}$ glasses. $\alpha = 33$ nm^{-1}.

Nominal	Log A [$(\Omega - m)^{-1}$ K$^{1/2}$]	B ($K^{1/4}$)/2.303	$N(E_F)$ ($\times 10^{21}$ eV^{-1}/cm^3)
$z = 0.4$	24.896	123.818	1.23
$z = 0.5$	20.492	97.234	3.22
$z = 0.6$	18.229	85.796	5.32
$z = 0.7$	21.078	95.732	3.43
$z = 0.8$	21.264	95.164	3.51

[**]$\sigma T^{1/2} = A \exp(-B/T^{1/4})$ $N(E_F) = (2.882 \times 10^{29})/(\text{slope})^4$ eV-1/cm^3

given by

$$\sigma = A \operatorname{Exp}(-B/T^{1/4}) \tag{6}$$

where

$$A = [e^2/2(8\pi)^{1/2}]\nu_o[N(E_F)/\alpha k_B T]^{1/2} \tag{7}$$

$$B = 4[2\alpha^3/9\pi k_B N(E_F)]^{1/4} \tag{8}$$

where ν_o is optical phonon frequency and α is the decay of the localized state wave function, $N(E_F)$ is the density of state at the Fermi level. Figure 7 shows plots of Log σ versus $T^{-1/4}$ and it is observed that the plots are linear over almost the whole temperature range of measurements consistent with the Mott VRH model. Equation (6) was fitted to the experimental data and the values of A and B calculated from these fits are given in Table 5. The values of $N(E_F)$ were calculated
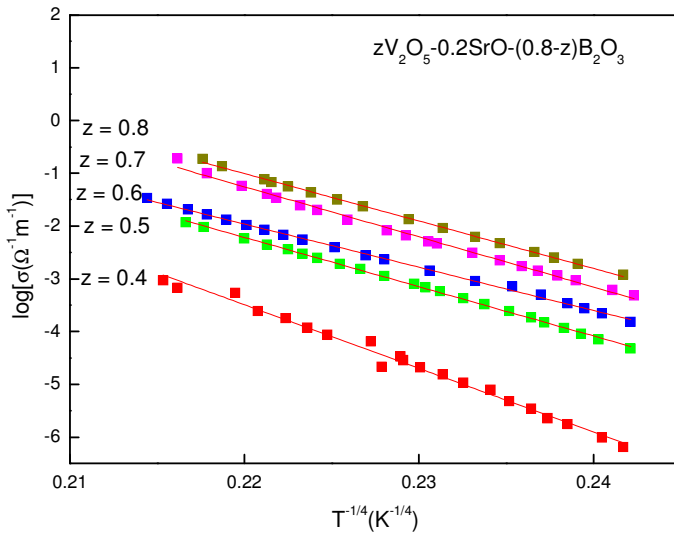
Fig. 7.   A plot of Log σ versus $T^{-1/4}$ for SrO-borovanadate $(V_2O_5)_z(SrO)_{0.2}(B_2O_3)_{0.8-z}$ glasses. The solid lines are best fits to Eq. (6).

Table 5. Parameters A, B, $N(E_F)$ obtained for Mott's variable-range hopping and percolation model** for SrO-borovanadate $(V_2O_5)_z(SrO)_{0.2}(B_2O_3)_{0.8-z}$ glasses. $\alpha = 33$ nm^{-1}.

Nominal	Log A $[(\Omega - m)^{-1}]$	B (K$^{1/4}$)/2.303	$N(E_F)$ ($\times 10^{21}$ eV$^{-1} \cdot$ cm^{-3})
$z = 0.4$	23.035	120.574	1.27
$z = 0.5$	18.343	93.446	3.52
$z = 0.6$	16.076	81.989	5.93
$z = 0.7$	19.638	94.972	3.29
$z = 0.8$	18.786	89.960	4.09

**$\sigma = A \exp(-B/T^{1/4})$ $N(E_F) = 2.68 \times 10^{29}/(\text{slope})^4$ eV^{-1}/cm^3

from Eq. (7). These values, shown in Table 5, are comparable with the values obtained for the vanadate glasses formed with traditional network former and the other semiconducting glasses.[31,32]

The values for $N(E_F)$ as well as those of A and B obtained from models (i) and (ii) are almost the same (differ by $\pm 8\%$ for $N(E_F)$ and less than $\pm 2\%$ for A and B, on the average) as shown in Tables 4 and 5 because these two models are modified form of Eq. (3) and in different parameters ranges. Both the models are suitable to explain our conductivity data.

(iii) Schnakenberg's polaron hopping model: a polaron hopping model, where $W_D \neq 0$, has been considered by Schnakenberg.[33] In this model, the optical multiphonon hopping process determines the dc conductivity at high temperature, while at low temperatures the conductivity is determined by the acoustical single phonon assisted hopping process. In this model, the expression for dc conductivity as a
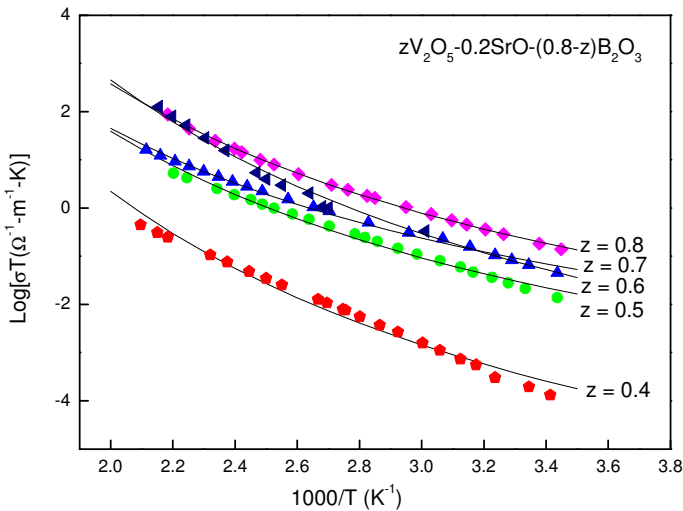
Fig. 8.   Best fits (solid curves) of the Schnakenberg model [Eq. (9)] to the experimental data for SrO-borovanadate $(V_2O_5)_z(SrO)_{0.2}(B_2O_3)_{0.8-z}$ glasses as plots of Log (σT) versus 1000/T.

Table 6.   Parameters obtained by fitting the dc conductivity data to the Schnakenberg model for SrO-borovanadate $(V_2O_5)_z(SrO)_{0.2}(B_2O_3)_{0.8-z}$ glasses.

Nominal	$\nu_o \times 10^{13}$ (s^{-1})	W_H (eV)	W_D (eV)	$W_H + W_D/2$ (eV)
$z = 0.4$	0.31	0.15	0.002	0.15
$z = 0.5$	0.38	0.13	0.004	0.13
$z = 0.6$	0.32	0.11	0.004	0.11
$z = 0.7$	0.32	0.10	0.003	0.10
$z = 0.8$	0.18	0.06	0.001	0.06

function of temperature is given by

$$\sigma = A/T[\sinh(h\nu_o/k_BT)]^{1/2}\text{Exp}[-(4W_H/h\nu_o)\tanh(h\nu_o/4k_BT)]\text{Exp}(-W_D/k_BT) \tag{9}$$

Equation (9) predicts a temperature dependent hopping energy which decreases with an increase of temperature consistent with the data presented in Fig. 3. Figure 8 shows plots of Log (σT) versus 1000/T and the *DC* conductivity has been fitted to the theoretical values given by this model [Eq. (9)]. W_H, W_D and ν_o were used as variable parameters in the fitting process and the best fits of the data have been obtained for the values of the parameters shown in Table 6. The values of ν_o are close to the values previously reported.[28] However, this model yields high values of W_H than the values of the activation energy estimated for the temperature range of measurements (Table 3). Further, $W_H + W_D/2$ is not equal to W (Table 3) and so is not in accordance with the prediction of the Mott model.[23,25]

4. Conclusion

The overall features of XRD patterns confirm the amorphous nature of the present glasses. The IR results agree with previous investigations on similar glasses and it has been concluded that with the introduction of B_2O_3 into SrO-vanadate glasses, the B atoms would substitute into the V sites of the various VO_n polyhedra and not result in any additional structural units. Upon the B_2O_3 concentration exceeding the SrO content, a third grouping is realized as BO_n structures, such as metaborate chain structures, BO_4 polyhedra, or $Sr_2B_2O_5$ units, are formed in boron rich regions in the borovandate glass network in addition to the VO_n polyhedra and SrV_2O_6 structures. Thus this qualitative picture of the local glass structure evolving as the relative concentration varies in these SrO-vanadate and SrO-borovanadate glasses is very similar to the interpretation of the glass structure based on the previous IR and EXFAS studies on these glasses. The temperature dependence of DC electrical conductivity of SrO-vanadate and SrO-borovandate glasses has been studied in terms of different hopping models. The data suggests that the conduction mechanism in the present glasses is due to non-adiabatic hopping of the polarons. Further, analysis of the conductivity data shows that the conductivity data are consistent

with Mott's nearest neighbor hopping model. Both Mott VRH and Greaves models are suitable to explain the data. The values of $N(E_F)$ obtained from the two models are consistent with each other and with those reported in the literature. Schnakenberg's generalized polaron hopping model is consistent with the temperature dependence of the activation energy but the various model parameters such as density of states, hopping energy, obtained from the best fits were found to be not in accordance with the prediction of the Mott model.

Acknowledgments

References

1. G. S. Linsley, A. E. Owen and F. M. Hayatee, *J. Non-Cryst. Solids* **4**, 208 (1970).
2. N. F. Mott, *J. Non-Cryst. Solids* **1**, 1 (1968).
3. I. G. Austine and N. F. Mott, *Adv. Phys.* **18**, 41 (1969).
4. A. W. Dozier, L. K. Wilson, E. J. Friebele and D. L. Kinser, *J. Am. Ceram. Soc.* **55**, 373 (1972).
5. B. S. Rawal and R. K. Maccrone, *J Non-Cryst. Solids* **28**, 347 (1978).
6. R. A. Montani, M. Levy and J. L. Souquet, *J. Non-Cryst. Solids* **149**, 249 (1992).
7. A. Ghosh and B. K. Chaudhuri, *J. Non-Cryst. Solids* **103**, 83 (1988).
8. G. D. Khattak, N. Tabet and L. E. Wenger, *Phys. Rev. B* **72**, 104203 (2005).
9. B. K. Sharma, D. C. Dube and A. Mansingh, *J. Non-Cryst. Solids* **65**, 39 (1984).
10. Y. Hakamatsuka, N. Yoneda and T. Tsuchiya, *Yogyo Kyokai Shi* **90**, 48 (1962).
11. V. Dimitrov, Y. Dimitriev, M. Arnaudov and D. Topalov, *J. Non-Cryst. Solids* **57**, 147 (1983).
12. E. Dachille and R. Roy, *J. Am. Ceram. Soc.* **42**, 78 (1965).
13. G. D. Khattak and A. Mekki, to be published.
14. M. J. Krogh, *J. Phys. Chem. Glasses* **6**, 46 (1965).
15. A. H. Verhoef and H. W. den Hartog, *J. Non-Cryst. Solids* **146**, 267 (1992).
16. E. I. Kamitsos, M. A. Karakassides and G. D. Chryssikos, *J. Phys. Chem. Glasses* **91**, 1073 (1987).
17. T. Hubert, G. Mosel and K. Witke, *Glass Phys. Chem.* **27**, 114 (2001).
18. O. Attos, M. Massot, M. Balkanski, E. Haro-Poniatowski and M. Asomoza, *J. Non-Cryst. Solids* **210**, 163 (1997).
19. T. Hubert, U. Harder, G. Mosel and K. Witke, in *Borate Glasses, Crystals, and Melts II*, eds. A. C. Wright, S. A. Feller and A. C. Hannon (Society of Glass Technology, Sheffield, 1997), p. 156.
20. H. Doweidar, A. Megahed and I. A. Gohar, *J. Phys. D: Appl. Phys.* **19**, 1939 (1986).
21. M. Sayer and A. Mansingh, *Phys. Rev. B* **6**, 4629 (1972).
22. A. Al-Hajry, A. Al-Shahrani and M. M. El-Desoky, *Mater. Chem. Phys.* **95**, 300 (2006).
23. A. E. Owen, *Progress in Ceramic Science*, Vol. 3 (Pergamon, Oxford, 1963), p. 350.
24. T. N. Kennedy and J. D. Mackenzie, *Phys. Chem. Glasses* **8**, 169 (1967).
25. N. F. Mott, *Philos. Mag.* **19**, 835 (1969).
26. C. H. Chung, J. D. Mackenzie and L. Murawski, *Rev. Chem. Miner.* **16**, 308 (1979).
27. G. N. Greaves, *J. Non-Cryst. Solids* **11**, 427 (1973).

28. S. Sen and A. Ghosh, *J. Phys.: Condens. Matter* **11**, 1529 (1999).
29. M. M. El-Desoky and I. Kashif, *Phys. Stat. Sol. (a)* **194**, 89 (2002).
30. A. Al-Shahrani, A. Al-Hajri and M. M. El-Desoki, *Phys. Stat. Sol. (a)* **300**, 378 (2003).
31. N. F. Mott and E. A. Davis, *Electronic Processes in Non-Crystalline Materials*, 2nd edn. (Clarendon, Oxford, 1979).
32. A. Ghosh, *Phys. Rev. B* **42**, 5665 (1990).
33. J. Schnakenberg, *Phys. Stat. Solidi* **28**, 623 (1968).